TITLE PAGE

Title: Cilastatin attenuates cisplatin-induced proximal tubular cell damage

Authors: Sonia Camano[*], Alberto Lazaro[*], Estefania Moreno-Gordaliza, Ana M. Torres, Carmen de Lucas, Blanca Humanes, Jose A. Lazaro, M. Milagros Gomez-Gomez, Lisardo Bosca, Alberto Tejedor

Laboratory of origin: Renal Physiopathology Laboratory, Department of Nephrology, Hospital General Universitario Gregorio Marañón, Madrid, Spain

Affiliations:

Renal Physiopathology Laboratory, Department of Nephrology, Hospital General Universitario Gregorio Marañón, Madrid, Spain (SC, AL, AMT, CL, BH, JAL, AT)**,** Department of Analytical Chemistry, Faculty of Chemistry, Universidad Complutense, Madrid, Spain (EMG, MMGG),

Instituto de Investigaciones Biomedicas Alberto Sols (CSIC-UAM), Madrid, Spain (LB)

JPET Fast Forward. Published on April 30, 2010 as DOI: 10.1124/jpet.110.165779
This article has not been copyedited and formatted. The final version may differ from this version.

JPET # 165779

RUNNING TITLE PAGE

Running title: Cilastatin reduces cisplatin-induced nephrotoxicity

Corresponding Author:

Dr. Alberto Tejedor.

Renal Physiopathology Laboratory, Department of Nephrology,

Hospital General Universitario Gregorio Maranon.

C/ Dr. Esquerdo 46, 28007, Madrid, Spain.

Tel: 34-91-4265145. Fax: 34-91-5868214.

E-mail: atejedor@senefro.org

Number of Text Pages: 38

Number of Figures: 9

Number of References: 37

Number of words: **Abstract**-- 241

Introduction-- 565

Discussion-- 1240

Abbreviations: RPTECs, renal proximal tubule epithelial cells; OCT, organic cation transporter; DHP-I, dehydrodipeptidase I; CyA, cyclosporine A; MTT, 3-(4, 5-dimethylthiazol-2-yl)- 2,5-diphenyltetrazolium bromide; $\Delta\psi m$, mitochondrial transmembrane potential; CFU, colony-forming units; Pt, platinum; SEC, size exclusion; ICP-MS, inductively coupled plasma mass spectrometry; LDH, lactate dehydrogenase; Fas-L, Fas-ligand; RPLPO, Ribosomal phosphoprotein large PO subunit

Recommended section: Gastrointestinal, Hepatic, Pulmonary, and Renal

ABSTRACT

A major area in cancer therapy is the search for protective strategies against cisplatin-induced nephrotoxicity. We investigated the protective effect of cilastatin on cisplatin-induced injury to renal proximal tubular cells. Cilastatin is a specific inhibitor of renal dehydrodipeptidase-I, which prevents hydrolysis of imipenem and its accumulation in the proximal tubule. Primary cultures of proximal cells were treated with cisplatin (1-30 μM) in the presence or absence of cilastatin (200μg/ml). Apoptosis and mitochondrial injury were assessed by different techniques. Cisplatin uptake and DNA binding was measured by inductively coupled plasma spectrometry. HeLa cells were used to control the effect of cilastatin on the tumoricidal activity of cisplatin. Cisplatin increased cell death, apoptotic like-morphology, caspase activation and mitochondrial injury in proximal tubular cells in a dose and time-dependent way. Concomitant treatment with cilastatin reduced cisplatin-induced changes. Cilastatin also reduced the DNA-bound platinum but did not modify cisplatin dependent upregulation of death receptors (Fas) or ligands (TNFα, Fas-L). In contrast, cilastatin did not show any effects on cisplatin-treated HeLa cells. Renal dehydrodipeptidase I was virtually absent in HeLa cells. Cilastatin attenuates cisplatin-induced cell death in proximal tubular cells without reducing the cytotoxic activity of cisplatin in tumor cells. Our findings suggest that the affinity of cilastatin for renal dipeptidase makes this effect specific for proximal tubular cells and may be related to a reduction in intracellular drug accumulation. Therefore, cilastatin administration might represent a novel strategy in the prevention of cisplatin-induced acute renal injury.

INTRODUCTION

Cisplatin (*cis*-diammine-dichloroplatinum II) is one the most potent antineoplastic drugs used for the treatment of many types of tumor (Boulikas and Vougiouka, 2003). Even though its mechanism of activity has not been clearly established, it is accepted that cisplatin blocks DNA replication and gene transcription by inducing breaks in single-and double-stranded DNA (Servais et al., 2008).

The tumoricidal activity of cisplatin is dose-dependent. In head and neck carcinoma, cisplatin as monotherapy at doses of 100-120 mg/m^2 every 3-4 weeks has a response rate of 19% (Liverpool Head and Neck Oncology group, 1990). At 200 mg/mm^2, it achieves response rates of 83% in previously untreated patients (Havlin et al., 1989). Nevertheless, cisplatin has potentially lethal adverse effects. The most common is nephrotoxicity (25-40% of treated patients), which limits its use and effectiveness in cancer therapy (Yao et al., 2007). The glomerular filtration rate can fall by 30% after only 2 doses, and treatments must often be stopped (Go and Adjei, 1999). In fact, only 60% of patients complete 3 out of 4 cisplatin cycles.

Cisplatin-induced nephrotoxicity involves enhanced oxidative stress, inflammatory reactions, and tubular cell apoptosis (Yao et al., 2007; Pabla and Dong, 2008; Lieberthal et al., 1996). Several pathways—including extrinsic and intrinsic pathways and the endoplasmic reticulum—are involved in proximal tubular apoptosis (Pabla and Dong, 2008). Several studies have demonstrated that cisplatin directly activates pro-apoptotic Bcl-2 family proteins such as Bax and Bak in cultured tubular cells and *in vivo* (Wei et al., 2007; Park et al., 2002), thus leading to mitochondrial permeability transition, release of cytochrome c, and activation of caspase 9, which finally activates caspase 3, the principal enzyme responsible for apoptosis of renal tubular cells.

Although several *in vitro* and *in vivo* approaches have been proposed to reduce cisplatin-induced nephrotoxicity (Wu et al., 2005; Nagothu et al., 2005; Jiang et al., 2007; Lee et al., 2009), the protection they provide is never complete, thus highlighting the need for combined strategies. However, it is unclear whether such approaches would limit the tumoricidal efficacy of cisplatin in cancer cells.

We took advantage of the way in which cisplatin is excreted by the kidney to design a strategy specifically aimed at inhibiting apical uptake of cisplatin by renal proximal tubular epithelial cells (RPTECs), without affecting its accumulation and effectiveness in other cells.

Although cisplatin is a substrate of organic cation transporter (OCT) 2 in the basolateral membrane of the proximal tubules, 60% of cisplatin administered is recovered from lysosomes on the apical membrane, indicating a major role of vesicle cycling in accumulation in RPTECs (Binks and Dobrota, 1989). The relative importance of the roles of the apical and basolateral pathways for the entry of cisplatin into proximal cells can be deduced by analyzing data from the non-filtering kidney (Binks and Dobrota, 1989).

The apical pole of RPTECs contains proteins found only at this location and which are probably involved in apical vesicle trafficking and extrinsic signal transduction. Inhibition of renal dehydrodipeptidase I (DHP-I), which is located on brush-border cholesterol rafts (Parkin et al., 2001), effectively reduces toxic intracellular accumulation of imipenem (Norrby et al., 1983), cyclosporine A (CyA), and tacrolimus (Tejedor et al., 2007; Perez et al., 2004), and provides specific RPTECs protection against apoptosis induced by these agents. In the present study we show that cilastatin, a specific inhibitor of brush border–bound renal DHP-I, can provide organ-specific protection against cisplatin-induced nephrotoxicity.

METHODS

Chemicals

Cisplatin was obtained from Pharmacia (Barcelona, Spain).

Crystalline cilastatin, kindly provided by Merck Sharp & Dohme S.A. (Madrid, Spain), was dissolved in cell culture medium at the specified concentrations. A dose of 200 µg/ml was chosen because it is cytoprotective and falls within the reference range for clinical use (Perez et al., 2004).

Proximal tubular primary cell culture and HeLa cell line culture

Porcine RPTECs were obtained as previously described (Perez et al., 2004). Briefly, the cortex was sliced and incubated for 30 minutes at 37°C with 0.6 mg/ml of collagenase A (Boehringer Mannheim, Germany) in Ham's F-12 medium. Digested tissue was then filtered through a metal mesh (250 µm), washed 3 times with Ham's F-12 medium, and centrifuged using an isotonic Percoll gradient [45% (v/v)] at 20,000*g* for 30 minutes. Proximal tubules were recovered from the deepest fraction, washed, and resuspended in supplemented DMEM/ Ham's F-12 in a 1:1 ratio (with 25 mM HEPES, 3.7 mg/ml sodium bicarbonate, 2.5 mM glutamine, 1% non-essential amino acids, 100 U/ml penicillin, 100 mg/ml streptomycin, 5 x 10^{-8} M hydrocortisone, 5 mg/ml ITS, and 2% fetal bovine serum). Proximal tubules were seeded at a density of 0.66 mg/ml and incubated at 37°C in a 95% air/5% CO_2 atmosphere. Culture medium was renewed every 2 days. RPTECs were used after they had reached confluence (80%).

HeLa cells were cultured in DMEM medium supplemented with 10% fetal bovine serum and 1% penicillin/streptomycin in a humidified environment with 95% air/5% CO_2 at 37ºC.

Cell death studies

Cell morphology: To detect evidence of apoptosis, cell morphology was observed using phase-contrast microscopy.

Nuclear staining: Cell nuclei were visualized following DNA staining with the fluorescent dye DAPI (Sigma-Aldrich, Missouri, USA). Briefly, cells were seeded on cover slips in a 24-well plate, fixed in 4% formaldehyde for 10 minutes and permeabilized with 0,5% Triton X-100. Cells were then rinsed with PBS, incubated with DAPI (12.5µg/ml) for 15 minutes and excess dye removed. Cell imaging was performed with the 40X PL-APO 1.25 NA oil objective of a Leica-SP2 confocal microscope (Leica Microsystems, Heidelberg, Germany). DAPI was excited with a 405 nm laser-diode. Emission between 420-490 nm was collected following Leica recommendations. Six fields with ~200 cells per field were examined in each condition to estimate the percentage of nuclei with apoptosis-like appearance.

Propidium iodide flow cytometry and cell detachment quantification: RPTECs were cultured with 30µM cisplatin in the presence or absence of cilastatin (200µg/ml) for 24 hours. Non-adherent and adherent cells were harvested separately and both cell populations were resuspended in 2% paraformaldehyde in PBS for 30 min at 4°C. Cells were washed with PBS, permeabilized with PBS–Tween 0.5% for 15 min at room temperature and incubated with 250µg/ml RNase and 40µg/ml propidium iodide (Sigma, USA) for 45 min at room temperature (Perez et al., 2004). Assay samples were analysed by flow cytometry with a FACScan equipped with a single argon ion laser (Becton Dickinson, Oxforf, UK) using standard Lysis II software. Detached cells were quantified by flow cytometry (FACScan). Side scatter, forward scatter and FL2-fluorescence were collected. FL2-A and FL2-W were used to identify and exclude doublets from the analysis.

JPET Fast Forward. Published on April 30, 2010 as DOI: 10.1124/jpet.110.165779
This article has not been copyedited and formatted. The final version may differ from this version.

Nucleosomal quantification: To evaluate DNA fragmentation in the context of apoptosis, RPTECs were incubated under specific conditions for 24 hours. At the end of this period RPTECs were lysed and centrifuged at 200 *g* for 10 min to remove cell debris. DNA and histones present in the soluble fraction were quantified using an enzyme-linked immunosorbent assay cell death kit (Boehringer Mannheim, Germany). Histone and DNA present in mono and oligo-nucleosomes in the cytoplasmic fraction of cell lysates were detected by a sandwich-enzyme immunoassay with antihistone and anti-DNA-peroxidase antibodies as previously described (Perez et al., 2004).

Caspase activity assay: Caspase-3, caspase 8 and caspase 9 activities were determined using the substrates DEVD-*p*NA, IETD-*p*NA and LEHD-*p*NA respectively, following the protocols of the APOPCYTO Caspase-3, Caspase-8 and Caspase-9 Colorimetric Assay Kits from MBL (Naka-ku Nagoya, Japan). At 24 or 48 hours of treatment, both adherent and non-adherent cells were harvested, resuspended in 120 µL of lysis buffer (MBL) and incubated at 4ºC for 10 minutes followed by centrifugation at 10 000 g for 5 minutes. Aliquots (50 µL) of supernatants were removed and placed in a 96-well microplate. Substrate was added, and the microplate was incubated at 37ºC for 2 hours. *p*NA light absorption was quantified using a spectrophotometer plate reader at 405 nm and compared with a linear standard curve generated on the same microplate.

Measurement of annexin V-FITC staining: Annexin staining was determined using confocal microscopy. RPTECs were treated for 12, 24 or 48 hours with 30µM cisplatin in the presence or absence of cilastatin (200µg/ml). Both adherent and non-adherent cells were collected and centrifuged 1 500 rpm 5 minutes, rinsed twice with binding buffer (10 mM Hepes, pH 7.4, 140 mM NaCl, 2.5 mM $CaCl_2$), resuspended at a final density of 1-2 x 10^6 cells/ml and incubated with 5 µl of annexin V-FITC (Biotium, Inc,

JPET Fast Forward. Published on April 30, 2010 as DOI: 10.1124/jpet.110.165779
This article has not been copyedited and formatted. The final version may differ from this version.

Hayward, CA) for 15 minutes at room temperature in the dark. Next, cells were fixed in 2% formaldehyde for 15 minutes at room temperature, washed and placed on a glass coverslip to be visualized. Microscopy was performed using a Leica-SP2 confocal microscope (Leica Microsystems). Different measurements of annexin V-FITC fluorescence were assessed with the Leica Confocal Software LCS-1537 (Leica Microsystems, Heidelberg, Germany).

Determination of LDH release: LDH release from RPTECs was measured in the culture media after treatment with cisplatin in the presence or absence of cilastatin (200µg/ml) for 24 and 48 hours. LDH was measured automatically in a modular auto-analyzer Cobas 711 (Roche Farma, Madrid, Spain). LDH release was expressed in relative terms to total LDH released by treatment with 0.1% Triton X-100 (100% release).

Cell viability assay: Cell survival assay relies on the capacity of cells to reduce 3-(4, 5-dimethylthiazol-2-yl)-2, 5-diphenyltetrazolium bromide (MTT) (Calbiochem, CA, USA) to colored formazan in metabolically active cells. RPTECs or HeLa cells were seeded and incubated with cisplatin alone or in combination with cilastatin. Twenty-four, forty-eight or seventy-two hours later, 0.5 mg/ml of MTT was added, and plates were incubated for 3 hours in the dark at 37ºC, and 100 µL of 50% dimethylformamide in 20% SDS (pH 4.7) was added. Plates were incubated at 37ºC overnight, and absorbance was measured at 595 nm. All assays were performed in triplicate.

Cell viability: Quantification of colony-forming units (CFU)

RPTECs were treated for 24 hours with cisplatin in the presence or absence of cilastatin (200µg/ml). Adherent cells were washed in saline serum, harvested with trypsin-EDTA, seeded in Petri dishes (100 mm), and cultured for 7 days in drug-free

complete medium. Surviving adherent cells were fixed for 5 minutes with 5% paraformaldehyde/PBS and stained with 0.5% crystal violet/20% methanol for 2 minutes. Excess dye was rinsed with PBS. Finally, the intracellular dye was eluted with 50% ethanol/50% sodium citrate 0.1 M (pH 4.2) and quantified by spectrometry at 595 nm.

Mitochondrial membrane potential assay

Changes in mitochondrial transmembrane potential ($\Delta\Psi m$) were measured using the JC-1 Assay Kit for Flow Cytometry (MitoProbe™, Molecular Probes, OR, USA) according to the manufacturer's protocol. JC-1 is a cationic dye that exhibits potential-dependent accumulation in mitochondria, indicated by a fluorescence emission shift from green (~529 nm) to red (~590 nm). Consequently mitochondrial depolarization is seen as a shift to lower JC-1 red fluorescence accompanied by an increase in JC-1 green fluorescence.

Data analyses were performed using WinMDI software by measuring both the green (530 ± 15 nm) and red (585 ± 21 nm) JC-1 fluorescence with a FACScan equipped with a single argon ion laser, (Becton Dickinson, UK). At least 10,000 events were acquired per sample. The membrane potential disruptor, carbonyl cyanide 3-chlorophenylhydrazone (CCCP, supplied with the kit, 50 µM final concentration) was used as a positive control.

Cytochrome c release

Release of cytochrome c from mitochondria into cytosol was measured using Western-blot analysis. RPTECs treated for 24 hours with 10-30µM cisplatin in the presence or absence of cilastatin (200 µg/ml) were harvested, washed once with ice-

JPET Fast Forward. Published on April 30, 2010 as DOI: 10.1124/jpet.110.165779
This article has not been copyedited and formatted. The final version may differ from this version.

cold PBS, and gently lysed for 10 minutes in ice with 90 µL of lysis buffer (250 mM sucrose, 80 mM KCl, 500 µg/ml digitonin, 1 mM DTT, 0.1 mM PMSF, and protease inhibitors in PBS). Cell lysates were centrifuged at 12,000*g* at 4ºC for 5 minutes to obtain the supernatants (cytosolic extract free of mitochondria) and the pellets (fractions containing the mitochondria), which were resuspended in 90 µL of lysis buffer. Equal amounts of protein were loaded (50 µg in each lane) and electrophoresed on 15% polyacrylamide gels as previously described (Gallego-Delgado et al., 2006).

Goat polyclonal antibody against C-terminus of cytochrome c of human origin (Santa Cruz Biotechnology, Inc, CA, USA) was used at 1:500. The membranes were also probed with goat polyclonal antibody against a peptide of VDAC1 of human origin (1:500; Santa Cruz Biotechnology, Inc) for mitochondrial fractions and monoclonal anti-α-tubulin Clone B-5-1-2 Mouse Ascites Fluid (mouse IgG1 isotype) antibodies (1:10,000; Sigma-Aldrich, Missouri, USA) for cytosolic fractions as internal controls for the technique. Proteins were visualized with the enhanced chemiluminescence detection system (ECL, Amersham, Buckinghamshire, UK).

Cellular cisplatin uptake and estimation of DNA-bound platinum. Platinum-biomolecule speciation analysis

RPTECs incubated for 24 hours with increasing concentrations of cisplatin in the presence or absence of cilastatin (200 µg/ml) were scraped and lysed in 400 µL of lysis buffer at 70ºC (2.22% [w/v] SDS; 19.33 % [v/v] glycerol [87% v/v]; 790 mM Tris HCl pH 6.8 in dH_2O, PMSF, and protease inhibitors). Cell lysates were heated at 100ºC for 5 minutes, homogenized in ice and centrifuged at 12 000*g* for 5 minutes at 4ºC. The supernatant was analyzed for total protein content, and cisplatin (as platinum-Pt-). Alternatively, for DNA-Pt measurements, RPTECs and HeLa cells were treated for 24

hours with cisplatin in the presence or absence of cilastatin (200 µg/ml) and both non-adherent cells and adherent cells were collected, rinsed with PBS and centrifuged at 13 000 rpm for 10 minutes. Cell pellet was resuspended in PBS /lysis buffer (v/v, 20 mM EDTA pH 8, 0.5% Triton X-100, 5 mM Tris pH 8) and incubated 30 minutes at 37ºC with 10 mg/ml RNase A (Invitrogen, Carlsbad, CA). Samples were then treated with proteinase K (10 mg/ml, Applied Biosystems, Ambion, Foster City, CA) at 55ºC for 3 hours and then extracted with phenol (equilibrated with Tris pH 8.0, Sigma-Aldrich) by shaking gently for 2 minutes. After centrifugation (12 000 rpm), the phases were separated, and the aqueous phase was isolated. The extraction was repeated twice with phenol-chloroform:isoamylalcohol (1-24:1, v/v) and finally with chloroform:isoamylalcohol (24:1, v/v). The DNA in the aqueous phase was precipitated by the addition of 100% ethanol at -20ºC and 3 M sodium acetate (pH 5.3) followed by incubation overnight at -80ºC. The DNA was collected by centrifugation (12 000 rpm, 15 minutes), washed with 1 ml of 70% ethanol, dried and resuspended in 300µL of 10mM Tris pH 7.6, 0.1 mM EDTA in sterile water. The DNA was quantitatively estimated from the absorption at 260 nm by using a NanoDrop UV-Vis instrument (Nucliber, Madrid, Spain).

Pt content in cell soluble fraction or DNA was measured using a Quadrupole Thermo X-series inductively coupled plasma mass spectrometer (ICP-MS) (Thermo Electron Windsford, Cheshire, UK) equipped with a Meinhard nebulizer, a Fassel torch, and an Impact Bead Quartz spray chamber cooled by a Peltier system. Prior to the analysis, samples were 5-fold diluted in aqueous solutions containing 2% HCl, which made it possible to stabilize Pt. Quantification was performed by external calibration; the internal standard was Ir, added in a final concentration of 20 µg /L to both samples and standards.

JPET Fast Forward. Published on April 30, 2010 as DOI: 10.1124/jpet.110.165779
This article has not been copyedited and formatted. The final version may differ from this version.

ICP-MS measurements were acquired in continuous mode, monitoring *m/z* ^{194}Pt, ^{195}Pt, and ^{191}Ir, and results were expressed as [µg Pt/g protein] and [µg Pt/g DNA]. *Pt-biomolecule speciation analysis*: Pt-biomolecules were analyzed by HPLC-ICP-MS. Supernatants were chromatographically separated using a Size Exclusion (SEC) Superdex 75 10/300 column, GL Pharmacia (Amersham), which presents a nominal separation at between 3 and 70 kDa. 10 mM Tris-NO_3, 25 mM NaCl (pH 7.42) was used as the mobile phase, at a flow rate of 0.8 ml/min. The SEC column was coupled to an ICP-MS and ^{195}Pt was monitored. Samples were 1:1 diluted with the mobile phase prior to analysis, and 100 µL of each sample was injected into the chromatographic system through a 0.22 µm nylon filter. In parallel, the SEC column was calibrated using several proteins with different molecular weights: blue dextran (>2000 kDa), bovine serum albumin (66 kDa), carbonic anhydrase (29 kDa), cytochrome c (12.4 kDa) and aprotinin (6.5 kDa) (Sigma–Aldrich Chemie), with a UV-vis detector. These molecular weights can be used as a reference for the separation capacity of the column, although it should be borne in mind that secondary interactions with the stationary phase could alter retention times.

Dehydrodipeptidase I and IV activity assays.

RPTECs or HeLa cells were incubated overnight with Gly-Phe-*p*-nitroanilide (DHP-I substrate, Sigma) 1mM in PBS for DHP-I activity determination, or with Gly-Pro-*p*-nitroanilide (DHP-IV substrate, Sigma) 1mM for DHP-IV activity determination. Both activities were measured in the presence or absence of cilastatin (200µg/ml). *P*-nitroanilide was quantified in aliquots from supernatants by measuring 410nm absorbance.

JPET Fast Forward. Published on April 30, 2010 as DOI: 10.1124/jpet.110.165779
This article has not been copyedited and formatted. The final version may differ from this version.

Cisplatin-induced expression of apoptotic genes in RPTECs

TNFα, Fas and Fas-L gene expression were analyzed by real-time PCR. RPTECs were cultured with 30μM cisplatin in the presence or absence of cilastatin (200μg/ml) for 24 hours. Total RNA was isolated by Trizol® method (Invitrogen) from RPTECs and processed according to the protocol provided by the manufacturer. In brief, 1 μg of RNA was reverse-transcribed with High Capacity cDNA Archive Kit (Applied Biosystems, Foster City, CA). Real time PCR was performed on a TaqMan ABI 7700 Sequence Detection System (Applied Biosystems) using heat-activated *Taq* DNA polymerase (Amplitaq Gold) (Lazaro A et al., 2005). For all quantitative cDNA analysis, the ΔCT technique was applied (Lazaro A et al., 2005). Ribosomal phosphoprotein large PO subunit (RPLPO) served as housekeeping gene and was amplified in parallel with the genes of interest. The expression of each target gene was normalized to RPLPO. Primers sequences for porcine TNFα, Fas, Fas-L and RPLPO were synthesized commercially (Invitrogen) and are available on request. All measurements were performed in duplicate. Controls consisting of ddH_2O were negative in all runs.

Immunofluorescence localization of Fas-L

RPTECs grown on sterile crystal coverslips were treated with 30μM cisplatin in presence or absence of cilastatin (200μg/ml) for 0.5 and 2 hours. Cells were washed with PBS and fixed in 4% formaldehyde in PBS for 10 minutes. Cells were washed twice in PBS and blocked for 1 hour in BSA 1%-PBS-Tween 0.1% at 37ºC. After, cells were incubate with rabbit polyclonal antibody against a peptide of C-terminus of Fas-L of human origin (1:50; Santa Cruz Biotechnology) for 1 hour at 37ºC followed by incubation with FITC-conjugated secondary antibody (Donkey anti-rabbit, 1:200; Jackson ImmunoResearch Laboratories, Inc., West Grove, PA, USA) in blocking

solution for another hour at 37ºC. Cell nuclei were counterstained with DAPI (5µg/ml Sigma-Aldrich). The absence of primary antibody was the negative control. After washing, cells were mounted in fluorescent mounting medium (Dako, Carpinteria, CA, USA) and Fas-L immunolocalization was examined with the 20X PL-APO 0.7 NA objective of a Leica-SP2 confocal microcope (Leica Microsystems). Different intensity measurements were assessed with the Leica Confocal Software LCS-1537 (Leica Microsystems).

Statistical methods

Quantitative variables were summarized as the mean± standard error of the mean (SEM). Differences were considered statistically significant for bilateral alpha values under 0.05. Factorial ANOVA was used when more than 1 factor was considered. When a single factor presented more than 2 levels, a post-hoc analysis (least significant difference) were performed, if the model showed significant differences between factors. When demonstrative results are shown, they represent a minimum of at least 3 repeats. When possible, a quantification technique (e.g. densitometry, dye recovery) has been used to illustrate reproducibility.

RESULTS

Cilastatin reduces cisplatin-induced proximal tubular cell death

Cisplatin induces time and dose-dependent cell death on primary culture of RPTECs. When RPTECs are exposed to increasing concentrations of cisplatin for 3, 6, 24 and 48 hours, direct observation by phase microscopy shows cell rounding and detachment from the plate. Cilastatin significantly reduced the observed impact for every cisplatin concentration and exposure time studied (Figure 1A).

However, cisplatin-induced cell death causes an early detachment of damaged cells from the plate. We studied the characteristics of non-adherent cells in terms of size, complexity and propidium iodide staining by flow cytometry after 24 hours exposition to increasing doses of cisplatin ± cilastatin. Figure 1B shows the flow cytometry histogram for propidium iodide staining (FL2-H) of non-adherent cells from control plates, 30μM cisplatin treated plates or 30μM cisplatin plus cilastatin treated plates. A relevant span of PI fluorescence was observed due to the fact that both diploid and hypodiploid populations are recovered in the supernatant. Figure 1C is a quantification of these non-adherent cells. Cilastatin caused a 70% reduction in cell detachment when 30μM cisplatin was used. Cell protection becomes statistically significant at cisplatin concentrations over 10μM.

Qualitative estimation of apoptotic cell death was obtained in adherent cells stained with DAPI (Figure 1D). Incubation with 30μM cisplatin led to cell shrinkage with significant nuclear condensation, fragmentation and formation of apoptotic like bodies (see arrows). Figure 1E shows a quantification of apoptotic nuclei in adherent cells. Cilastatin reduced nuclear damage by 64%.

We quantified the functional impact of cisplatin treatment on cell survival by measuring the % of adherent cells still able to reduce MTT to formazan after exposition to increasing doses of cisplatin. Coincubation with cilastatin doubles cell survival in every condition analyzed. Statistical significations were obtained for incubations with cilastatin in 10µM cisplatin and more than 24 hours (Figure 2A).

Analysis of nucleosomal DNA fragmentation and migration from nuclei to cytosol is presented in figure 2B. RPTECs exposed to cisplatin for 24 hours present a dose-dependent increase in nucleosomes recovered from cytosol, which were reduced by cilastatin treatment.

To better characterize the apoptosis process triggered on RPTECs by cisplatin we quantified annexin V-FITC staining and caspase 3, 8 and 9 activation. Cisplatin caused an increase in annexin V-FITC staining that reached a maximum at 24 hours and persisted till 48 hours (Figure 2C). Confocal microscopy demonstrated that annexin V was mainly localized to the outer leaflet of the plasma membrane (data not shown). Cilastatin coincubation showed a lesser annexin V staining, with a reduction of 53% (Figure 2C). Since apoptosis is generally followed by secondary necrosis, which is associated with the leakage of plasma membrane, we also measured the release of LDH from the cells in the medium (figure 2D). At 24 hours, 30µM cisplatin incubation caused a 6% release of total LDH cellular content (as estimated from Triton X-100 treatment). This percentage rose to a 30% at 48 hours. Interestingly, necrotic cell death was not modified by cilastatin coincubation, indicating that cilastatin reduction of cisplatin-induced cell death was specific for apoptosis. Cisplatin induced apoptosis was further confirmed by caspase 9, 8 and 3 activities. Figure 3A, B and C, show that increasing doses of cisplatin caused significant activation of caspase 8 and 3, being caspase 9 less evident. Cilastatin reduced caspase 8 and caspase 3 activations at 24 and

48 hours (for caspase 3, figure 3D). Cilastatin alone had no effect on any of the previously reported data.

Cilastatin reduces cisplatin-induced mitochondrial damage

Mitochondrial damage is a central event in the cytotoxic and nephrotoxic activity of cisplatin. Comparison of control cells with cisplatin-treated RPTECs, showed evident membrane depolarization (decrease in red fluorescence; FL2-H) with no changes in green fluorescence (FL-1H) (Figure 4A). Cilastatin alone did not have a significant effect on $\Delta\psi m$. However, cilastatin partially prevented $\Delta\psi m$ loss when RPTECs were simultaneously exposed to cisplatin and cilastatin. The results were quantified and expressed in relative terms compared to total depolarization induced by CCCP (Figure 4B).

To further investigate the role of the mitochondria in cilastatin-mediated effect, cisplatin action with and without cilastatin on cytochrome c release was studied. As presented in Figure 4C, the subcellular distribution of cytochrome c between mitochondria (particulate) and cytosol reveals a significant degree of protection, indicating that cilastatin improves the cell viability of RPTECs (Figure 4C and 4D).

Cilastatin improves long-term recovery and cell viability in RPTECs after exposure to cisplatin

To know the long-term viability of surviving RPTECs after 24-hour exposure to cisplatin, we tested the ability of those cells to proliferate into new cell colonies.

CFU were quantified as specified in Methods. The CFU count fell dramatically after 24 hours of treatment with cisplatin, and this fall was clearly dose-dependent (Figure 5A). When RPTECs were exposed to cisplatin and cilastatin simultaneously,

JPET Fast Forward. Published on April 30, 2010 as DOI: 10.1124/jpet.110.165779
This article has not been copyedited and formatted. The final version may differ from this version.

the number of CFU was significantly greater after 7 days of recovery at every cisplatin concentration studied. The intracellular dye was extracted and absorbance quantified at 595 nm (Figure 5B).

Cilastatin reduces intracellular accumulation of cisplatin. Effects in DNA-bound Pt

The nephrotoxicity of cisplatin is largely dependent on the intracellular concentration reached, more specifically on the DNA-bound Pt. Dose-dependent cisplatin accumulation was measured in the soluble fraction of RPTECs after 24 hours incubation (Figure 6A). Because of the early cell detachment detected previously, we decided also to quantify DNA-bound Pt in adherent cells as well as non-adherent cells, after 24 hours incubation with 30μM cisplatin (Figure 6B). Cilastatin caused a significant reduction (24%) in Pt recovered from cell soluble fraction, but the effect was much more relevant when DNA-bound Pt was analyzed in the presence of cilastatin; DNA-bound Pt was reduced by 55% in adherent cells and by 44% in non-adherent cells.

Speciation studies were performed by SEC-ICP-MS on RPTECs. As figure 6C shows, there is no change in the profile of Pt-containing proteins irrespective of whether or not cells are treated with cilastatin. Pt-bound proteins were observed within the whole separation range (3-70 kDa), and the most intense peaks corresponded to species around 70 and 7 kDa.

Moreover, no significant peaks were observed for intact cisplatin or the intracellular monoaquo complex, which elute at 47.3 and 30.6 min respectively, indicating that all the Pt is bound to biomolecules (Figure 6C).

JPET Fast Forward. Published on April 30, 2010 as DOI: 10.1124/jpet.110.165779
This article has not been copyedited and formatted. The final version may differ from this version.

Cell type specify of cilastatin protection: the case of HeLa cells

To evaluate the potential loss of the tumoricidal effect of cisplatin caused by the presence of cilastatin, we applied cisplatin to a tumor-derived cell line. When HeLa cells were exposed to increasing concentrations of cisplatin for 24 and 48 hours, a dose and time-dependent cell death was observed. Cilastatin have not any effect against the cisplatin-induced loss of cell viability (Figure 7A).We measured DNA-bound Pt both in adherent and non-adherent HeLa cells after 24 hours exposition to 30μM cisplatin. Pt concentration was double in non-adherent cells. As expected, cilastatin coincubation did not modify cisplatin binding to DNA (Figure 7B). To confirm the absence of DHP-I in HeLa cells, we measured the specific DHP-I activity on Gly-Phe dipeptides, and its sensitivity to cilastatin inhibition. Figure 7C shows the activity of cilastatin sensitive DHP-I activity in HeLa cells compared to RPTECs.

Effects of cisplatin and cilastatin in apoptotic gene expression in RPTECs

The reduction in DNA-bound Pt induced by cilastatin could be probably playing a role in the observed nephroprotection. However, it did not explain why only apoptotic but not necrotic linked processes were affected by cilastatin. In an attempt to establish if cilastatin interference with cisplatin death induction could be exclusively explained in terms of reduction in cell cisplatin availability, we decided to explore the gene expression of TNFα, Fas and Fas-L as mediators of apoptosis. Cisplatin increased TNFα and Fas mRNA in RPTECs at 24 hours, but in contrast it did not modify the level of Fas-L (real-time PCR, Figure 8). Cilastatin had no effect on the expression of any of the studied genes (Figure 8), suggesting that transcriptional changes were probably not relevant in cilastatin protection.

JPET Fast Forward. Published on April 30, 2010 as DOI: 10.1124/jpet.110.165779
This article has not been copyedited and formatted. The final version may differ from this version.

Effect of cisplatin and cilastatin in Fas-L distribution

We finally explored the possibility that cilastatin-DHP-I interaction could be related to the posttranscriptional induction of apoptosis by cisplatin. As caspase 3 and caspase 8 were actively induced by cisplatin, we decided to study if cilastatin modified other steps upstream in the extrinsic pathway of apoptosis. The expression and cell membrane localization of Fas-L was followed by confocal microscopy in RPTECs treated with 30μM cisplatin during very short periods of time. Fas-L was identified as specified in Methods. In Figure 9A, upper panels, Fas-L is identified on the cell surface after 30 minutes incubation, but it disappeared from the membrane after 2 hours. In the presence of cilastatin 200μg/ml, similar pattern was observed at 30 minutes. However, after 2 hours of treatment, Fas-L was still attached to the membrane, suggesting an interference with ligand sites internalization. Fas-L staining along the time was quantified in Figure 9B.

DISCUSSION

Cisplatin accumulation in renal cells causes nephrotoxicity, the main disadvantage of clinical use of cisplatin in oncology (Arany and Safirstein, 2003). The highest concentrations of cisplatin in the kidney are reached in the proximal tubule where toxicity is both time and dose-dependent (Yao et al., 2007; Ciarimboli et al., 2005). Proximal tubular cell death is considered the main pathophysiological mechanism underlying cisplatin nephrotoxicity, acute kidney injury and limiting factor for its clinical use (Pabla and Dong, 2008).

Renal tubular cell death after in vitro exposure to cisplatin has been well documented (Lieberthal et al., 1996; Park et al., 2002; Cummings and Schnellmann, 2002; Okuda et al., 2000). Direct observation of our primary cell cultures under treatment with cisplatin characteristically displayed apoptotic morphological changes that were fully consistent with previous observations (Park et al., 2002; Nagothu et al., 2005; Jiang et al., 2007; Okuda et al., 2000; Price et al., 2004).

In our primary cell culture of RPTECs, cisplatin causes a dose and time-dependent loss of cells. Although there is some necrosis as confirmed by LDH release to the medium, most of the cell deaths seem to be mediated by apoptosis activation. In proximal cells, cisplatin-induced apoptosis may follow both intrinsic and extrinsic pathways. As expected, RPTECs incubated in the presence of cisplatin presented severe mitochondrial damage observed in different ways, including loss of $\Delta\Psi m$, release of cytochrome c, and a diminished capacity to reduce MTT to formazan (Park et al., 2002; Nagothu et al., 2005). In our experimental set up, TNFα and Fas induction and caspase 8 and 3 activation suggest a relevant involvement of the extrinsic pathway, with persistent caspase activation after 48 hours of exposition. Damaged cells quickly loss the adherent properties.

In this study, we show that cilastatin, a specific inhibitor of tubular brush border DHP-I, attenuates cisplatin-induced nephrotoxicity *in vitro*, probably in more than one way.

At a concentration of 200μg/ml, cilastatin reduced cisplatin-induced caspase activation, cytochrome c release, membrane depolarization, nuclear condensation, DNA fragmentation, annexin V exposure, and ameliorated viability of surviving cells. Harvesting and reseeding surviving cells allows quantifying the number of CFU several days after the injury, and consequently the ability to restore a damaged tubule. Cilastatin not only reduced the initial damage to RPTECs, but also enabled surviving cells to undergo a better recovery.

We chose a concentration close to the expected plasma levels reached in humans treated with imipenem-cilastatin —200 μg/ml—even if it was not the most protective concentration. Cilastatin by itself had no significant effects on growth dynamics, cell confluence, or monolayer morphology of RPTECs (Perez et al., 2004).

Previous results from our group showed that cilastatin also reduced the toxicity of CyA and tacrolimus by inhibiting their transcellular transport and, consequently, their accumulation in the cell (Tejedor et al., 2007; Perez et al., 2004). Accordingly, we first hypothesize that cilastatin could be interfering with cisplatin intracellular accumulation.

Our results show that in the presence of cilastatin there was a modest dose-dependent reduction in cisplatin recovered from cell soluble fractions. However, cilastatin reduced significantly the amount of DNA-bound cisplatin in monolayer populations as well as in non-adherent cells. Cisplatin is known to permeate proximal tubular cells through apical and basolateral transporters (Miura et al., 1987; Endo et al., 2000), and there is recent evidence that both basolateral OCT 1 and 2 and copper transporter Ctr1 are involved in cisplatin transport, accumulation, and toxicity

(Ciarimboli et al., 2005; Pabla et al., 2009; Yokoo et al., 2007). In both cases, apoptosis and accumulation of cisplatin were decreased but not eliminated in the presence of competitive organic cations or transporter knockdown (Ciarimboli et al., 2005; Pabla et al., 2009; Yokoo et al., 2007). Once inside the cell, the relatively low intracellular chloride concentrations promote the dissociation of the chloride ions from the Pt molecule, thus increasing formation of the reactive, aquated species of cisplatin which readily interact with intracellular biomolecules (Daley-Yates and McBrien, 1985). Our analyses of intracellular Pt content and the Pt speciation studies on cisplatin-treated RPTECs in the presence or absence of cilastatin, showed that cilastatin significantly reduced cisplatin accumulation and DNA binding, but did not modify the chromatographic profile corresponding to Pt-containing biomolecules. This indicates that the identity of Pt-biomolecules in the cell is not altered. Therefore, it seems that entry of cisplatin in the cell is partially impaired after administration of cilastatin, with no changes in intracellular cisplatin metabolism.

On the other hand, cilastatin did not prevent cisplatin activation of genes of death like TNFα or Fas, and could not prevent or reduce necrotic cell death. Therefore, reduction in cisplatin intracellular accumulation or in binding DNA was possibly not the only mechanism behind nephroprotection, as no pretranscriptional effects were evident.

Caspase 8 and caspase 3 activation suggested a positive role for extrinsic pathway in the observed toxicity of cisplatin on RPTECs (Tsuruya K et al., 2003). Cilastatin first effect should be located in a step between cisplatin dependent genes induction (not modified by cilastatin) and caspase activation (reduced by cilastatin). Cilastatin affinity for membrane bound DHP-I made us focus to a potential interaction at the level of cell death receptors signalling. Cisplatin may induce very rapid Fas-clustering in the membrane lipid rafts of cancer cells and may trigger the apoptotic extrinsic cascade,

even in the absence of Fas-L (Dimanche-Boitrel et al., 2005). Trimerization of Fas seems to be a rate limiting step for the process. We have shown that Fas-L binding to the RPTECs membrane is clearly visible 30 minutes after cisplatin exposition, and 2 hours later Fas-L binding is not visible any more. This scenario changes when cilastatin is present: Fas-L binds cell membrane after 30 minutes of cisplatin exposition, but 2 hours later Fas-L is still binding the membrane surface, with no apparent processing. This interference could be causally related to reductions in caspase 8 and 3 activations, annexin V exposure, mitochondrial damage, cell detachment and nucleosomes formation observed when cilastatin is co-incubated with cisplatin.

Although the exact mechanism behind this interference is not clear yet, it was very relevant to know if other cell models without cilastatin target on their membranes would be or not protected by cilastatin against cisplatin toxicity. HeLa cells were our choice because of their tumor origin, the absence of brush border, and the virtual absence of DHP-I activity, this point being directly assessed by us. As expected, cisplatin did cause a sustained and dose dependent death on HeLa cells, as estimated by the progressive reduction in cell viability (MTT reduction capacity). However cilastatin did not modify any of these parameters, being not protective at all. DNA-bound cisplatin was not modified by cilastatin neither in monolayer nor in supernatants.

Cilastatin is a molecule specifically designed to inhibit brush border sorted DHP-I (Parkin et al., 2001; Garner et al., 2007). It is even probable that DHP-I is primarily located in apical cholesterol rafts (Pang S et al., 2004), nearby the Fas site (Dimanche-Boitrel MT et al., 2005). We do not know if DHP-I activity is necessary in the mediation of the apoptosis extrinsic signalization or if it is just an unwanted neighbour whose binding to cilastatin may cause a steric interference with the process.

The fact is that this work supports a new role for cilastatin in reducing cisplatin-induced nephrotoxicity. Identification of additional targets for cilastatin in this protective mechanism, together with currently available pharmacological data on cilastatin could enable us to develop potent therapeutic strategies for renal function preservation in cancer patients.

ACKNOWLEDGEMENTS

We would like to thank Dr. Rafael Samaniego for help with confocal microscopy, Dra. Paqui G. Traves for technical assistance with real-time PCR and Merck Sharp & Dohme for providing the cilastatin used in the study.

This work is dedicated to the memory of Remedios Fernández (1945-2009).

REFERENCES

Arany I and Safirstein RL (2003) Cisplatin nephrotoxicity. *Semin Nephrol* **23**: 460-464.

Aronoff GR, Bennett WM, and Berns JS, Brier ME, Kasbekar N, Mueller BA, Pasko DA and Smoyer WE (2007) *Drug Prescribing in Renal Failure. Dosing Guidelines for Adults and Children*, 5th ed. American College of Physicians, Versa Press, Philadelphia.

Binks SP and Dobrota M (1989) Distribution of platinum amongst the subcellular organelles of the rat kidney after oral administration of cisplatin, in *Nephrotoxicity. In vitro to in vivo animals to man* (Bach PH and Lock EA eds) pp 331-347, Plenum Press, New York.

Boulikas T and Vougiouka M (2003) Cisplatin and platinum drugs at the molecular level. *Oncol Rep* **10**: 1663-1682.

Ciarimboli G, Ludwig T, Lang D, Pavenstadt H, Koepsell H, Piechota HJ, Haier J, Jaehde U, Zisowsky J and Schlatter E (2005) Cisplatin nephrotoxicity is critically mediated via the human organic cation transporter 2. *Am J Pathol* **167**: 1477-1484.

Cummings BS and Schnellmann RG (2002) Cisplatin-induced renal cell apoptosis: caspase 3-dependent and -independent pathways. *J Pharmacol Exp Ther* **302**: 8-17.

Daley-Yates PT and McBrien DC (1985) A study of the protective effect of chloride salts on cisplatin nephrotoxicity. *Biochem Pharmacol* **34**: 2363-2369.

Dimanche-Boitrel MT, Meurette O, Rebillard A and Lacour S (2005) Role of early plasma membrane events in chemotherapy-induced cell death. *Drug Resist Updat* **8**: 5-14.

Endo T, Kimura O and Sakata M (2000) Carrier-mediated uptake of cisplatin by the OK renal epithelial cell line. *Toxicology* **146**: 187-195.

Gallego-Delgado J, Lazaro A, Gomez-Garre D, Osende JI, Gonzalez-Rubio ML, Herraiz M, Manzarbeitia F, Fortes J, Fernandez-Cruz A and Egido J (2006) Long-term organ protection by doxazosin and/or quinapril as antihypertensive therapy. *J Nephrol* **19**: 588-598.

Garner AE, Smith DA and Hooper NM (2007) Sphingomyelin chain length influences the distribution of GPI-anchored proteins in rafts in supported lipid bilayers. *Mol Membr Biol.* **24**: 233-42.

Go RS and Adjei AA (1999) Review of the comparative pharmacology and clinical activity of cisplatin and carboplatin. *J Clin Oncol* **17**: 409-422.

Havlin KA, Kuhn JG, Myers JW, Ozols RF, Mattox DE, Clark GM and von Hoff DD (1989) High-dose cisplatin for locally advanced or metastatic head and neck cancer. A phase II pilot study. *Cancer* **63**: 423-427.

Jiang M, Pabla N, Murphy RF, Yang T, Yin XM, Degenhardt K, White E and Dong Z (2007) Nutlin-3 protects kidney cells during cisplatin therapy by suppressing Bax/Bak activation. *J Biol Chem* **282**: 2636-2645.

Lazaro A, Gallego-Delgado J, Justo P, Esteban V, Osende J, Mezzano S, Ortiz A and Egido J (2005). Long-term blood pressure control prevents oxidative renal injury. Antioxid Redox Signal **7**:1285-93.

Lee KW, Jeong JY, Lim BJ, Chang YK, Lee SJ, Na KR, Shin YT and Choi DE (2009) Sildenafil attenuates renal injury in an experimental model of rat cisplatin-induced nephrotoxicity. *Toxicology* **257**: 137-143.

Lieberthal W, Triaca V and Levine J (1996) Mechanisms of death induced by cisplatin in proximal tubular epithelial cells: apoptosis vs. necrosis. *Am J Physiol* **270**: F700-F708.

Liverpool Head and Neck Oncology Group (1990) A phase III randomised trial of cisplatinum, methotrextate, cisplatinum + methotrexate and cisplatinum + 5-FU in end stage squamous carcinoma of the head and neck. *Br J Cancer* **61**: 311-315.

Miura K, Goldstein RS, Pasino DA and Hook JB (1987) Cisplatin nephrotoxicity: role of filtration and tubular transport of cisplatin in isolated perfused kidneys. *Toxicology* **44**: 147-158.

Nagothu KK, Bhatt R, Kaushal GP and Portilla D (2005) Fibrate prevents cisplatin-induced proximal tubule cell death. *Kidney Int* **68**: 2680-2693.

Norrby SR, Alestig K, Bjornegard B, Burman LA, Ferber F, Huber JL, Jones KH, Kahan FM, Kahan JS, Kropp H, Meisinger MA and Sundelof JG (1983) Urinary recovery of N-formimidoyl thienamycin (MK0787) as affected by coadministration of N-formimidoyl thienamycin dehydropeptidase inhibitors. *Antimicrob Agents Chemother* **23**: 300-30.

Okuda M, Masaki K, Fukatsu S, Hashimoto Y and Inui K (2000) Role of apoptosis in cisplatin-induced toxicity in the renal epithelial cell line LLC-PK1. Implication of the functions of apical membranes. *Biochem Pharmacol* **59**: 195-201.

Pabla N and Dong Z (2008) Cisplatin nephrotoxicity: mechanisms and renoprotective strategies. *Kidney Int* **73**: 994-1007.

Pabla N, Murphy RF, Liu K and Dong Z (2009) The copper transporter Ctr1 contributes to cisplatin uptake by renal tubular cells during cisplatin nephrotoxicity. *Am J Physiol Renal Physiol* **296**: F505-F511.

Pang S, Urquhart P and Hooper NM (2004) N-glycans, not the GPI anchor, mediate the apical targeting of a naturally glycosylated, GPI-anchored protein in polarised epithelial cells. *J Cell Sci*. **117**: 5079-86.

Park MS, De Leon M and Devarajan P (2002) Cisplatin induces apoptosis in LLC-PK1 cells via activation of mitochondrial pathways. *J Am Soc Nephrol* **13**: 58-865.

Parkin ET, Turner AJ and Hooper NM (2001) Differential effects of glycosphingolipids on the detergent-insolubility of the glycosylphosphatidylinositol-anchored membrane dipeptidase. *Biochem J* **358**: 209-216.

Perez M, Castilla M, Torres AM, Lazaro JA, Sarmiento E and Tejedor A (2004) Inhibition of brush border dipeptidase with cilastatin reduces toxic accumulation of cyclosporin A in kidney proximal tubule epithelial cells. *Nephrol Dial Transplant* **19**: 2445-2455.

Price PM, Safirstein RL and Megyesi J (2004) Protection of renal cells from cisplatin toxicity by cell cycle inhibitors. *Am J Physiol Renal Physiol* **286**: F378-F384.

Ross DA and Gale GR (1979) Reduction of the renal toxicity of cis-dichlorodiammineplatinum(II) by probenecid. *Cancer Treat Rep* **63**: 781-787.

Servais H, Ortiz A, Devuyst O, Denamur S, Tulkens PM and Mingeot-Leclercq MP (2008) Renal cell apoptosis induced by nephrotoxic drugs: cellular and molecular mechanisms and potential approaches to modulation. *Apoptosis* **13**: 11-32.

Tejedor A, Torres AM, Castilla M, Lazaro JA, de Lucas C and Caramelo C (2007) Cilastatin protection against cyclosporin A-induced nephrotoxicity: clinical evidence. *Curr Med Res Opin* **23**: 505-513.

Tsuruya K, Tokumoto M, Ninomiya T, Hirakawa M, Masutani K, Taniguchi M, Fukuda K, Kanai H, Hirakata H, Iida M. (2003) Antioxidant ameliorates cisplatin-induced renal tubular cell death through inhibition of death receptor-mediated pathways. Am J Physiol Renal Physiol **285**:F208-18.

Wei Q, Dong G, Franklin J and Dong Z (2007) The pathological role of Bax in cisplatin nephrotoxicity. *Kidney Int* **72**: 53-62.

Wu YJ, Muldoon LL and Neuwelt EA (2005) The chemoprotective agent N-acetylcysteine blocks cisplatin-induced apoptosis through caspase signaling pathway. *J Pharmacol Exp Ther* **312**: 424-431.

Yao X, Panichpisal K, Kurtzman N and Nugent K (2007) Cisplatin nephrotoxicity: a review. *Am J Med Sci* **334**: 115-124.

Yokoo S, Yonezawa A, Masuda S, Fukatsu A, Katsura T and Inui K (2007) Differential contribution of organic cation transporters, OCT2 and MATE1, in platinum agent-induced nephrotoxicity. *Biochem Pharmacol* **74**: 477-487.

FOOTNOTES

This work was supported by grants from the Fondo de Investigaciones Sanitarias [FIS-PI05/2259, PI08/1481]; MICINN [CTQ2008-04873/BQU, BFU2008-02161]; Comunidad de Madrid [CIFRA 0283/2006] and Fundacion Mutua Madrilena [TJ2BS].

SC and AL are recipients of a health care research contract from Comunidad de Madrid and FIS ("Sara Borrell"), respectively.

*These authors contributed equally to this work.

LEGENDS FOR FIGURES

Figure 1. Effects of cilastatin on renal proximal tubular epithelial cell (RPTEC) morphology during treatment with cisplatin. RPTECs were cultured in the presence of cisplatin (1, 10 and 30μM) and cisplatin + cilastatin (200μg/ml) for 24 hours. **A**, Phase-contrast photomicrographs are shown (representative example of at least three independent experiments; original magnification x40). **B**, Flow cytometry analysis: non-adherent cells were harvested fixed and stained with propidium iodide for DNA content. FL2-H signal is presented for the three estudied conditions. **C**, The effect of cilastatin on cisplatin-induced detachment of RPTECs, was measured by flow cytometry and determined by counting the number of cells in an equal volume of buffer. **D**, Nuclear staining with DAPI. Adherent RPTECs treated with cisplatin 30μM and cisplatin 30μM + cilastatin 200μg/ml, were stained with DAPI to study if apoptotic-like nuclear morphology was present. Arrows point to fragmented, apoptotic nuclei. **E, Q**uantitative approach to the images presented in **D**. Data are represented as the mean ± SEM of at least three separate experiments. ANOVA models $p<0.0001$.*$P< 0.05$, ***$P< 0.0001$ vs. control; ‡$P< 0.05$, †$P< 0.0001$ vs. same data without cilastatin.

Figure 2. Cilastatin attenuates cisplatin-induced apoptosis but not necrosis. Renal proximal tubular epithelial cells (RPTECs) were exposed to cisplatin (1, 10, and 30μM) and cisplatin + cilastatin (200μg/ml) for indicated times. **A**, Effect of cilastatin on cisplatin-induced loss of cell viability determined by the ability to reduce MTT (see Methods). Results are expressed as the percentage of the value obtained relative to control (without cisplatin and cilastatin). ANOVA model: $p<0.0001$; cisplatin dose: $p< 0.0001$, cilastatin effect: $p<0.0001$; time effect $p<0.0001$; cilastatin * time: NS. ***$P< 0.0001$ all data vs. control (except 30μM+cilastatin; 10μM+cilastatin; and

1μM±cilastatin at 24 hours, p= NS); †P< 0.0001 every condition + cilastatin vs. same condition without cilastatin (except 10μM+ cilastatin and 30μM + cilastatin at 24 hours, p<0.05) **B**, Oligonucleosomes at 24 hours were quantified in the cell soluble fraction and detected with an ELISA kit. **C,** Phosphatidylserine externalization was determined in non-adherent cells by annexin V-FITC staining and confocal microscopy quantification. **D,** Effect of cilastatin in cisplatin-induced LDH release. Data are presented as % of total LDH release obtained by Triton X-100 cell treatment. Data are represented as the mean ± SEM of at least three separate experiments. ANOVA models: p<0.0001. *P< 0.05, **P< 0.01, ***P< 0.0001 vs. control; ‡P< 0.05, †P< 0.0001 vs. same data without cilastatin.

Figure 3. Effect of cisplatin and cilastatin on caspase activity. A, **B** and **C** show the activation of caspase 9, caspase 8 and caspase 3 respectively with increasing doses of cisplatin for 24 hours, and the effect of cilastatin (200μg/ml). ANOVA model p<0.0001. **P< 0.01, ***P< 0.0001 vs. control; #P< 0.01, †P< 0.0001 vs. same data without cilastatin. **D**, Time course activation of caspase 3 with different doses of cisplatin ± cilastatin 200μg/ml**.** Data are represented as the mean ± SEM of four experiments.ANOVA model p<0.0001; cisplatin dose p<0.0001; cilastatin effect p<0.0001; cilastatin x cisplatin p<0.0001. **P< 0.01, ***P< 0.0001 vs. control; #P< 0.01, †P< 0.0001 vs. same data without cilastatin.

Figure 4. Effect of cilastatin on cisplatin-induced mitochondrial injury. A, Changes in mitochondrial membrane potential (ΔΨm) were analyzed by flow cytometry after staining with JC-1. Renal proximal tubular epithelial cells (RPTECs) were incubated with 30μM cisplatin with or without 200μg/ml cilastatin for 24 hours. Results are

presented as contour plots. **B,** Quantification of the results of 4 independent experiments. As a positive control, cells were treated for 5 minutes with 50 μM CCCP (carbonyl cyanide 3-chlorophenylhydrazone). Decrease in red fluorescence with CCCP was considered as 100% of the change in ΔΨm. Data are the mean ± SEM. ANOVA model $p<0.0001$. *$P< 0.05$ vs. control; ‡$P< 0.05$ vs. same data without cilastatin. **C,** Western blot analysis of cytochrome c of cytosolic and mitochondrial fractions of RPTECs treated with 10μM and 30μM cisplatin in the presence or absence of cilastatin 200μg/ml for 24 hours. VDAC and α-tubulin antibodies were used as internal loading controls for mitochondrial (particulate) and cytosolic fractions, respectively. Camptothecin (Campto) 50 μg/ml was used as a positive control. **D**, The values corresponding to normalized cytochrome c band intensity. Mean ± SEM of 3 separate experiments. ANOVA model $p<0.0001$. ***$p<0.0001$ compared with control group; ‡$p<0.05$, †<0.0001 vs. same data without cilastatin.

Figure 5. Cilastatin preserves long-term recovery of cisplatin-treated renal proximal tubular epithelial cells (RPTECs). A, RPTECs plated on six-well plates were incubated with 10μM and 30μM cisplatin in the presence or absence of cilastatin 200μg/ml for 24 hours. Cells were then trypsinized, washed, and seeded in Petri dishes in the presence of complete medium with 10% FBS, but without cisplatin or cilastatin, to allow for recovery. The number of colony-forming units was determined by staining with crystal violet after 7 days. Cilastatin increased the number of long-term surviving cell colonies. The photographs represent 3 different experiments. **B,** Quantification of crystal violet staining. Mean ± SEM of 3 experiments. ANOVA model $p<0.0001$. ***$P<0.0001$ vs. control; ‡$P< 0.05$, †$P<0.0001$ vs. same data without cilastatin.

Figure 6. Effects of cilastatin on cisplatin uptake and speciation analysis in renal proximal tubular epithelial cells (RPTECs). **A,** Platinum was measured in RPTECs soluble fractions using a Quadrupole inductively coupled plasma mass spectrometer (ICP-MS). RPTECs were treated with cisplatin in the presence or absence of cilastatin 200µg/ml for 24 hours. Values were expressed as the means ± SEM of platinum concentration expressed in µg Pt/g protein (n= 4 different experiments). ANOVA model p<0.0001; *cilastatin effect P< 0.05; ‡dose effect P<0.05. **B**, DNA-bound platinum was measured under the same conditions, using the same methods after DNA extraction from treated RPTECs. Data are presented as the mean ± SEM of 4 experiments. ANOVA model p<0.0001. ‡P< 0.05, †P<0.0001 vs. same data without cilastatin. **C**, Size Exclusion-ICP-MS (^{195}Pt signal) chromatograms from cytosols of RPTECs treated with cisplatin 10µM with or without cilastatin 200µg/ml for 24 hours. The main chromatographic peaks for the 2 samples present the same retention times and similar relative intensity. The graph represents 3 separate experiments.

Figure 7. Effect of cilastatin on the tumoricidal activity of cisplatin on HeLa cells. HeLa cells were treated with cisplatin alone (1, 10, 30µM) or in combination with cilastatin 200µg/ml. **A**, Loss of cell viability was determined at 24 and 48 hours by the ability to reduce MTT (see Methods). HeLa incubated in the absence of cisplatin and cilastatin was used as 100%. Values are expressed as the mean ± SEM of 4 different experiments. ANOVA model p<0.0001; effect of cisplatin p<0.0001; effect of cilastatin: NS; effect of time p<0.0001; cilastatin x cisplatin: NS; cilastatin x time: NS. **B**, DNA-bound platinum was measured in HeLa cells isolated DNA using a Quadrupole inductively coupled plasma mass spectrometer (ICP-MS). HeLa cells were treated with cisplatin 30µM in the presence or absence of cilastatin 200µg/ml for 24 hours. Values were expressed as the means ± SEM of platinum concentration expressed in µg Pt/g

DNA (n= 4 different experiments). **C**, Dehydrodipeptidase I specific activity (mU/mg x10^{-}3) in cultured RPTECs and HeLa. Activity was determined by the hydrolysis of 1 mM Gly-Phe-*p*-nitroanilide in the presence or absence of cilastatin 200µg/mL. P-nitroanilide absorbance was followed at 410 nm. *** P< 0.0001 vs. RPTECs.

Figure 8. Effects of cisplatin and cilastatin on mRNA expression of apoptotic genes in renal proximal tubular epithelial cells (RPTECs).

RPTECs were cultured in the presence of 30µM cisplatin and cisplatin + cilastatin (200µg/ml) for 24 hours. Expression of **A**, TNFα, **B**, Fas and **C**, Fas-L were analyzed by quantitative real-time PCR. Results as means± SEM of 4 separate experiments. ANOVA models p<0.0001. *P<0.05, ***P<0.0001 vs control.

Figure 9. Effects of cisplatin and cilastatin on immunofluorescence localization of Fas-L. Proximal tubular epithelial cells (RPTECs) were cultured on sterile coverslips and treated for the indicated time periods with 30µM cisplatin in the presence or absence of cilastatin (200µg/mL). **A**, Confocal microscopy images are a representative experiment of 3 immunofluorescence staining of Fas-L. **B,** A summary of the quantification of Fas-L fluorescence intensity is presented as means± SEM. ANOVA model: p<0.005; cilastatin effect p<0.001; time effect p<0.005; cilastain x time p<0.05. *P<0.05, **P<0.01 vs. control; #P< 0.01, ‡P< 0.05 vs. same data without cilastatin. Bar, 20 µm.

Figure 1

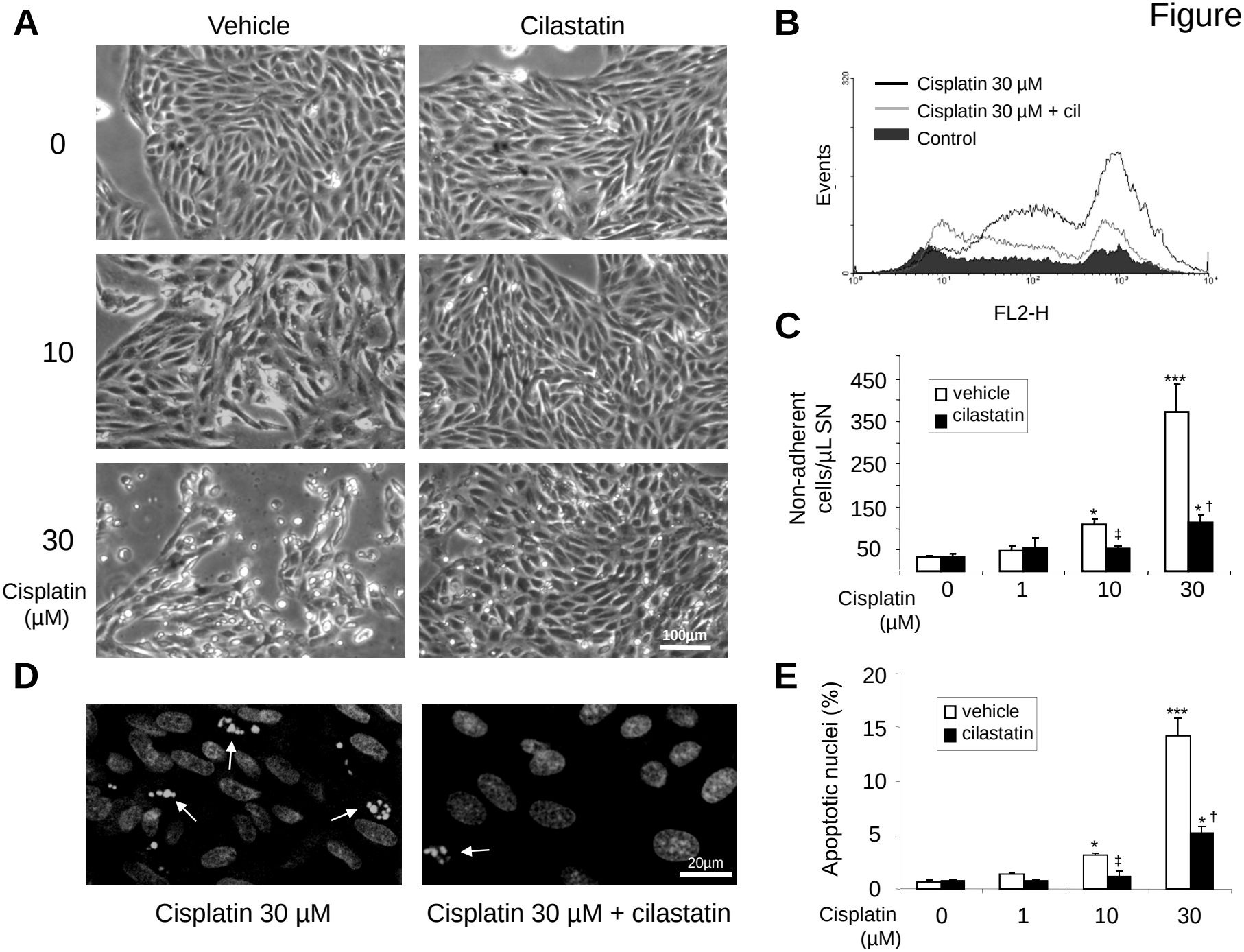

Figure 2

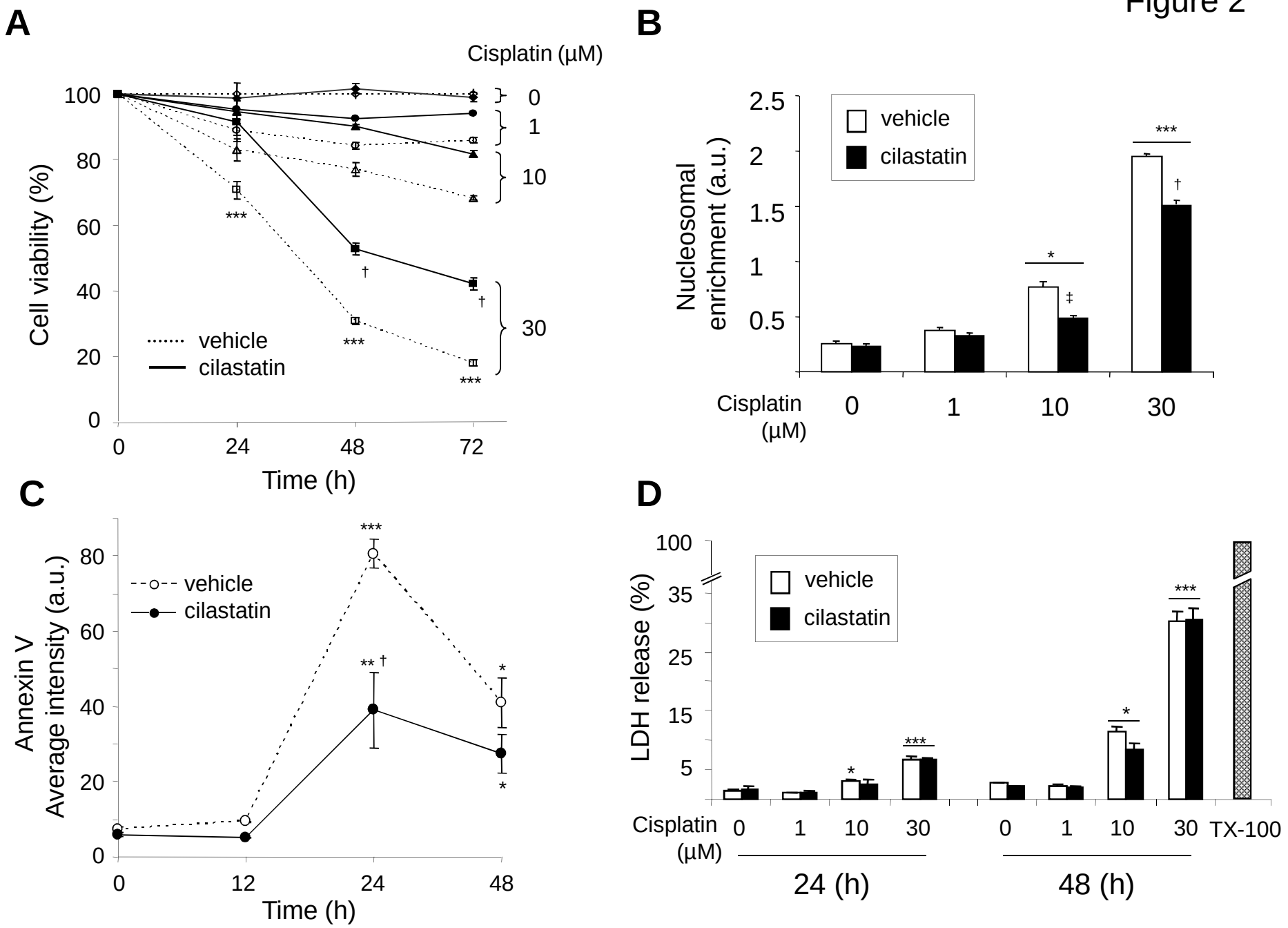

Figure 3

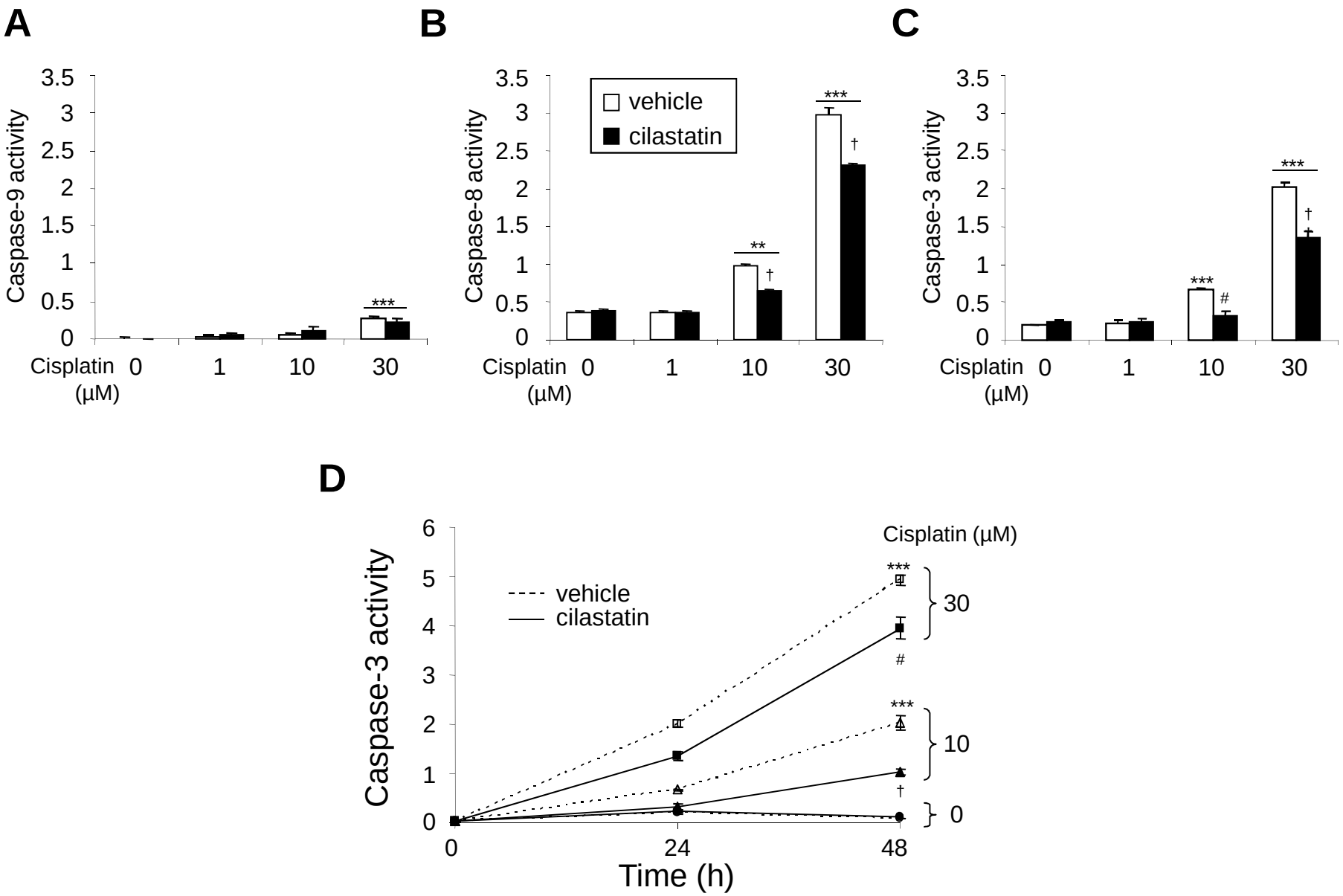

Figure 4

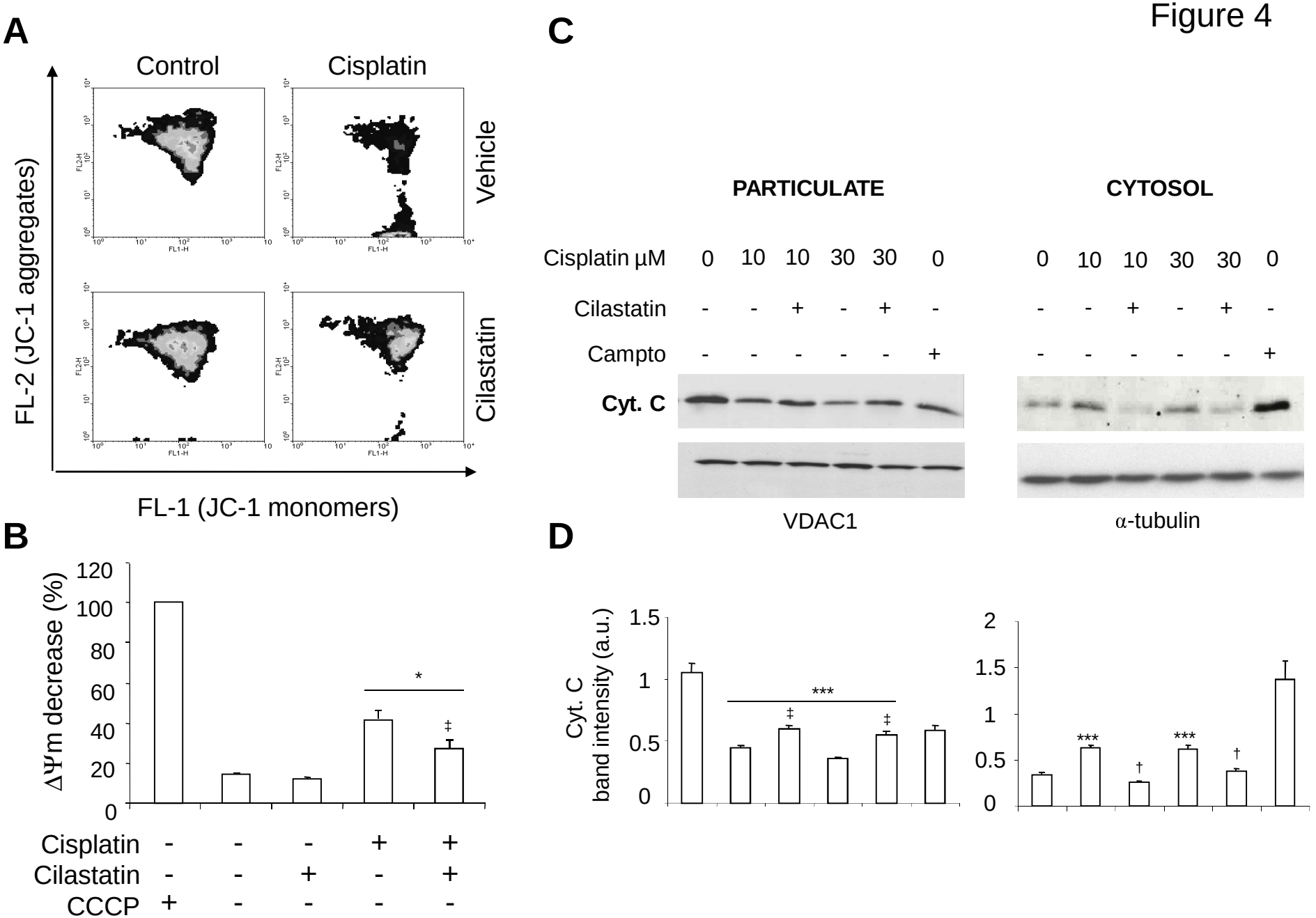

Figure 5

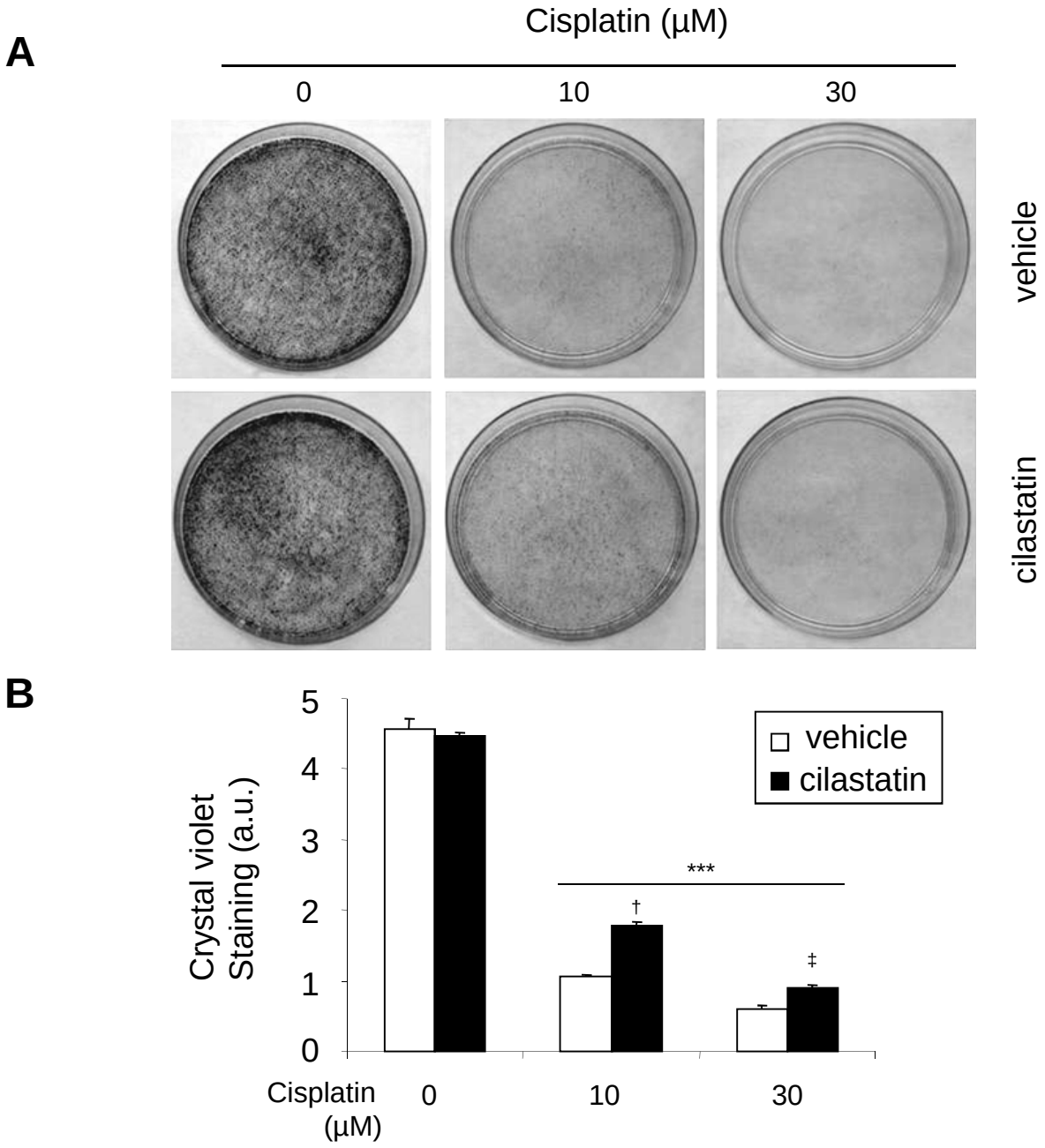

Figure 6

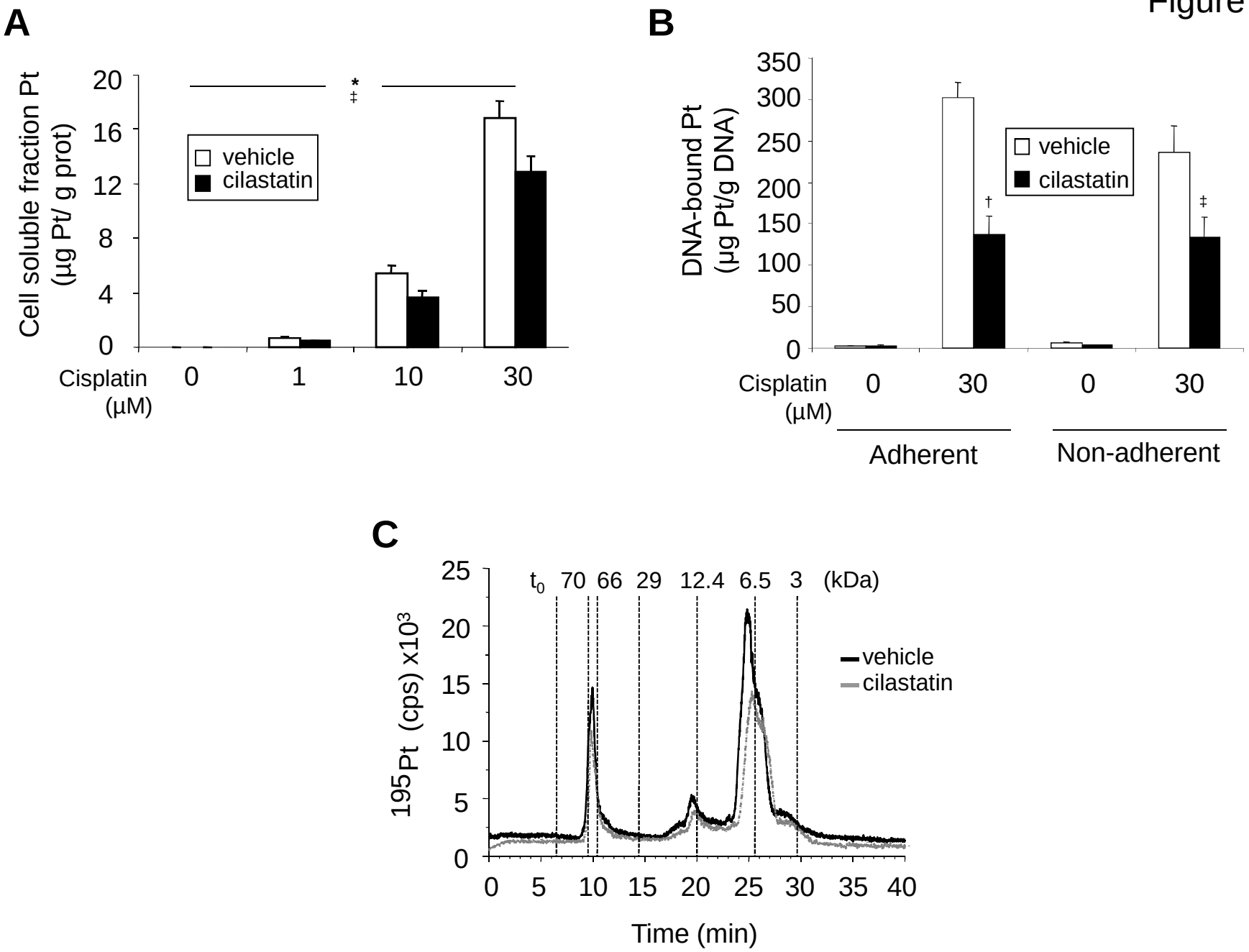

Figure 7

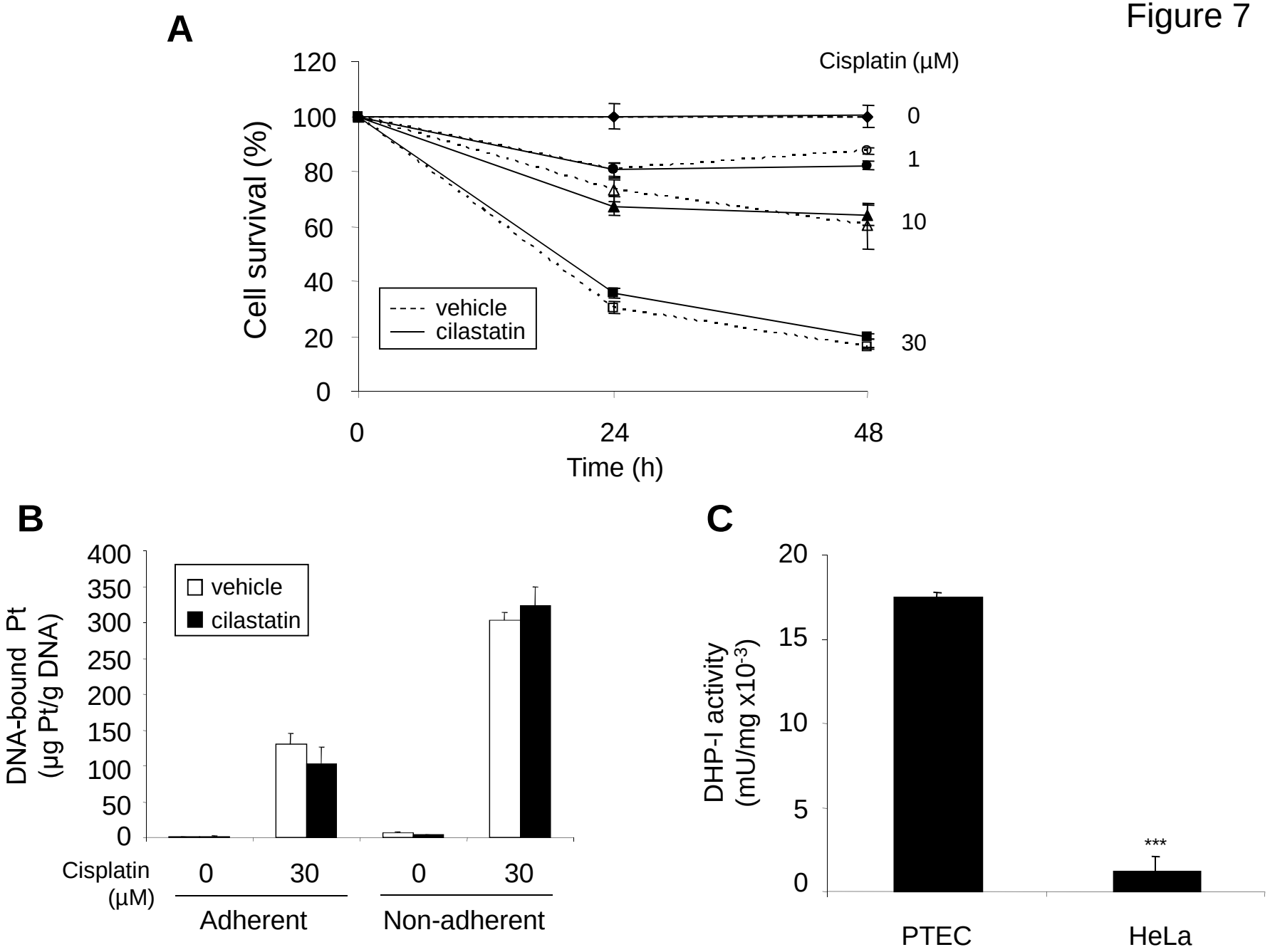

Figure 8

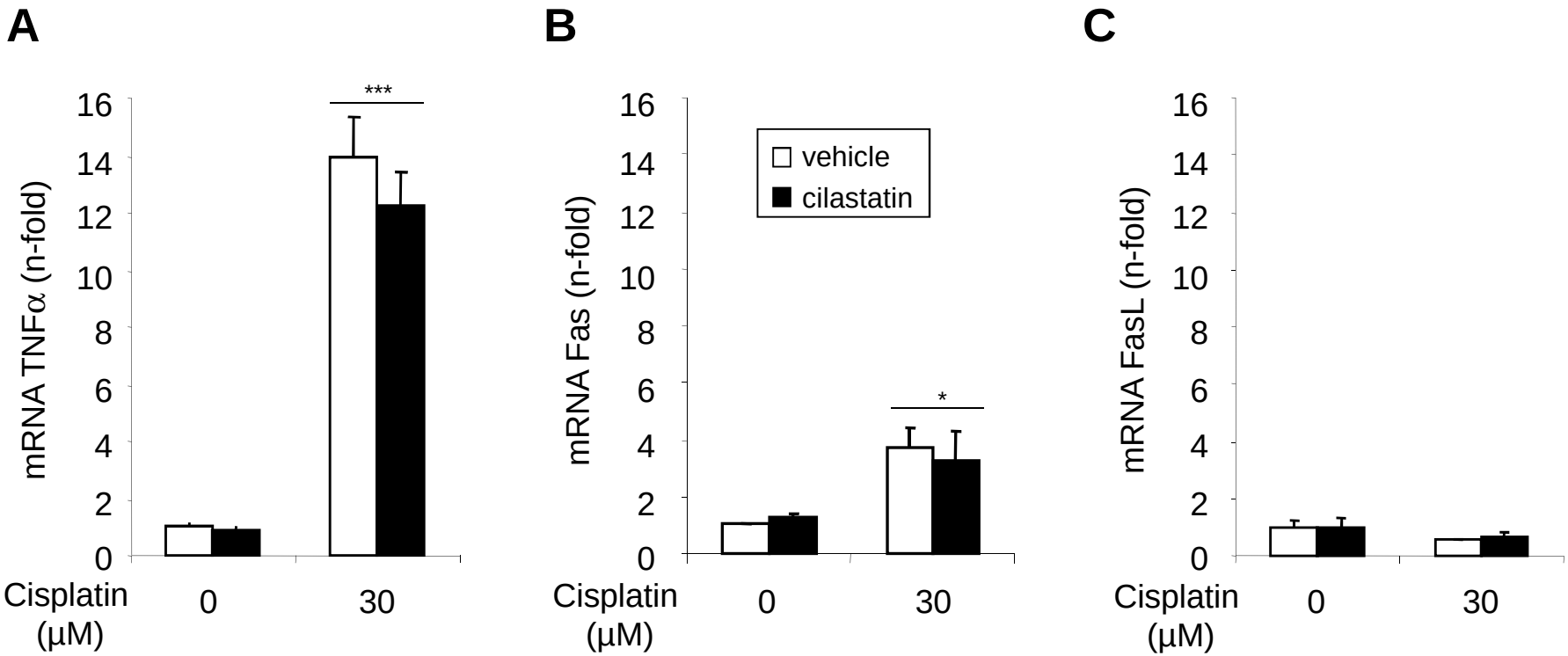

Figure 9